OXFORD

Comparative Effects of Bone Marrow-derived Versus Umbilical Cord Tissue Mesenchymal Stem Cells in an Experimental Model of Bronchopulmonary Dysplasia

Merline Benny[1,2], Benjamin Courchia[1,2], Sebastian Shrager[1,2], Mayank Sharma[1,2], Pingping Chen[1,2], Joanne Duara[1,2], Krystalenia Valasaki[3], Michael A. Bellio[3], Andreas Damianos[1,2], Jian Huang[1,2], Ronald Zambrano[1,2], Augusto Schmidt[1,2], Shu Wu[1,2], Omaida C. Velazquez[4], Joshua M. Hare[3,5], Aisha Khan[3], Karen C. Young[1,2,3,*,] (iD)

[1]Department of Pediatrics, University of Miami Miller School of Medicine, Miami, FL, USA
[2]Batchelor Children's Research Institute, University of Miami Miller School of Medicine, Miami, FL, USA
[3]The Interdisciplinary Stem Cell Institute, University of Miami Miller School of Medicine, Miami, FL, USA
[4]Department of Surgery, University of Miami Miller School of Medicine, Miami, FL, USA
[5]Department of Medicine, University of Miami Miller School of Medicine, Miami, FL, USA
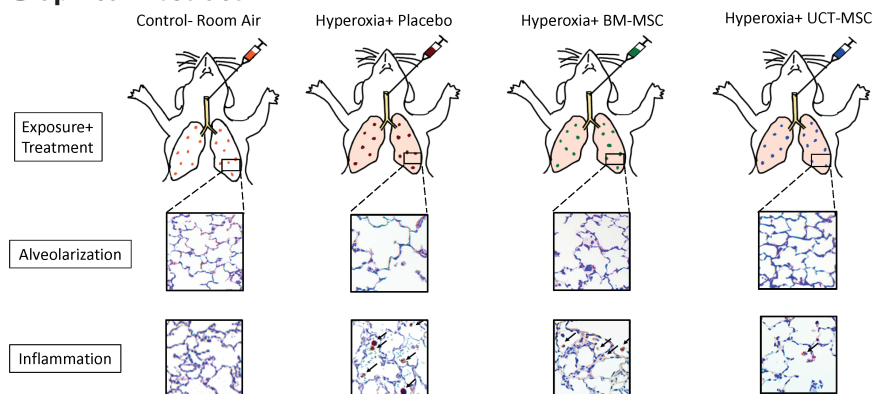
*Corresponding author: Karen C. Young, MD, Batchelor Children's Research Institute, University of Miami Miller School of Medicine, 1580 NW 10th Avenue, RM-345, Miami, FL 33136, USA. Tel: 305-243-4531; Email: Kyoung3@med.miami.edu

Abstract

Bronchopulmonary dysplasia (BPD) is a life-threatening condition in preterm infants with few effective therapies. Mesenchymal stem or stromal cells (MSCs) are a promising therapeutic strategy for BPD. The ideal MSC source for BPD prevention is however unknown. The objective of this study was to compare the regenerative effects of MSC obtained from bone marrow (BM) and umbilical cord tissue (UCT) in an experimental BPD model. In vitro, UCT-MSC demonstrated greater proliferation and expression of anti-inflammatory cytokines as compared to BM-MSC. Lung epithelial cells incubated with UCT-MSC conditioned media (CM) had better-wound healing following scratch injury. UCT-MSC CM and BM-MSC CM had similar pro-angiogenic effects on hyperoxia-exposed pulmonary microvascular endothelial cells. In vivo, newborn rats exposed to normoxia or hyperoxia (85% O_2) from postnatal day (P) 1 to 21 were given intra-tracheal (IT) BM or UCT-MSC (1×10^6 cells/50 µL), or placebo (PL) on P3. Hyperoxia PL-treated rats had marked alveolar simplification, reduced lung vascular density, pulmonary vascular remodeling, and lung inflammation. In contrast, administration of both BM-MSC and UCT-MSC significantly improved alveolar structure, lung angiogenesis, pulmonary vascular remodeling, and lung inflammation. UCT-MSC hyperoxia-exposed rats however had greater improvement in some morphometric measures of alveolarization and less lung macrophage infiltration as compared to the BM-MSC-treated group. Together, these findings suggest that BM-MSC and UCT-MSC have significant lung regenerative effects in experimental BPD but UCT-MSC suppresses lung macrophage infiltration and promotes lung epithelial cell healing to a greater degree.

Key words: cell therapy; mesenchymal stem cells; umbilical cord tissue; bone marrow; bronchopulmonary dysplasia.

Graphical Abstract

Control- Room Air   Hyperoxia+ Placebo   Hyperoxia+ BM-MSC   Hyperoxia+ UCT-MSC

Exposure+ Treatment

Alveolarization

Inflammation

Comparative Effects of Bone Marrow (BM) Derived versus Umbilical Cord Tissue (UCT) Mesenchymal Stem Cells (MSC) in an Experimental Model of Bronchopulmonary Dysplasia
BM-MSC and UCT-MSC have significant lung regenerative effects in experimental BPD but UCT-MSC suppress lung macrophage infiltration and promote lung epithelial cell healing to a greater degree.

Significance Statement

Bronchopulmonary dysplasia (BPD) is a significant health care problem. Mesenchymal stem/stromal cells (MSCs) may represent the next breakthrough therapy for BPD. However, there is a significant knowledge gap in the ideal source of MSC for BPD. Here, we demonstrate that bone marrow (BM) and umbilical cord tissue (UCT)-MSC improve the alveolar structure, vascular density, pulmonary hypertension, vascular remodeling, and lung inflammation in an experimental BPD model. However, there were trends for better alveolar protection and reduction in inflammation in UCT-MSC-treated animals. These findings have significant implications for cell therapy as MSC treatment for BPD moves from the bench to the bedside.

Introduction

Bronchopulmonary dysplasia (BPD), first described in 1967 by Northway et al remains one of the most common, complex, and intriguing complications of premature birth.[1] Advances in neonatal care have modified the phenotype of BPD, but the disease continues to be a significant health care burden, with few effective treatments. In the age of antenatal steroids, surfactant therapy, and noninvasive ventilation, BPD has evolved from a disease rooted in barotrauma to a multifactorial disease characterized by an arrest of alveolar and vascular development.[1] This unique paradigm shift in BPD has resulted in a drive to investigate innovative strategies to improve postnatal lung development.

Mesenchymal stem or stromal cells (MSCs) are a promising therapeutic strategy for BPD.[2] MSCs are easily expanded and readily isolated from accessible sources, such as bone marrow, adipose tissue, dental pulp, placenta, amniotic fluid, umbilical cord blood, and Wharton's Jelly.[3] Studies in our laboratory and others demonstrate that early administration of intra-tracheal (IT) bone marrow (BM)-derived MSC improves alveolarization, promote angiogenesis, reduce pulmonary hypertension (PH), and vascular remodeling in rodent models of BPD.[2,4-6] These benefits were primarily paracrine-mediated and secondary to MSC's potent anti-inflammatory and pro-angiogenic properties.[4,7,8] Investigations using umbilical cord blood (UCB)-derived MSC have also revealed that IT UCB-derived MSC improves lung function and survival in experimental BPD models.[9-11] UCB and umbilical cord tissue (UCT)-derived MSC are particularly attractive for therapy as they are easily harvested, more proliferative,[12] and potentially more immunomodulatory[13] as compared to BM-derived MSC. The yield of MSC in term UCB is however very low and isolation of these cells from term UCB has not always been successful.[12,14] UCT-derived MSC are isolated with significantly more efficiency than BM or UCB-derived MSC.[15] There is also emerging evidence that UCT-MSC has greater anti-inflammatory effects that are potentially due to differences in its expression of surface immunomodulatory molecules and cytokines.[13,16] UCT-MSC does not express CD80, CD40, or CD86, surface molecules involved in T lymphocyte activation.[17] They also have a higher expression of several anti-inflammatory cytokines than BM-derived MSC,[12,18,19] but whether they have superior lung regenerative effects in BPD has been less explored.

Here, we tested the hypothesis that UCT-derived MSC has superior lung-protective effects as compared to BM-MSC in neonatal rats with hyperoxia-induced lung injury, an experimental model of BPD.

Methods

MSC Culture and Characterization

MSCs were obtained from the BM of 18-45-year-old healthy male and female adults ($N = 3$) and UCT of healthy male and female term infants ($N = 3$). BM-MSC were isolated and expanded at the GMP Facility at the Interdisciplinary Stem Cell Institute of the University of Miami. We used freshly thawed MSC for the in vivo experiments. Briefly, bone marrow was processed by layering on top of Lymphocyte Separation Medium (Corning, Corning, NY) and centrifugation at $3000 \times g$ for 30 minutes to isolate the density-enriched, mononuclear cells. The mononuclear cells were then plated onto 175 cm² (Greiner bio-one Cellstar, Monroe, NC) for BM-MSC isolation through cell adhesion and expansion at a seeding density of 3.0×10^7 cells/flask. UCT-MSC were expanded from whole umbilical cords digested with 0.2% collagenase II solution (Worthington Biochemical Corporation, Lakewood, NJ) for 12-18 hours at 37°C under 5% CO_2. The homogenate was centrifuged ($500 \times g \times 10$ minutes) to pellet the cell suspension, washed 3 times with phosphate buffer solution (Corning, Corning, NY), and resuspended in culture media (alpha MEM GIBCO, Thermo Fisher Scientific, Waltham, MA) supplemented with 20% fetal bovine serum (Hyclone, Marlborough, MA), 1% penicillin/streptomycin, and 1% L-glutamine. Cells were cultured (37°C, 5% CO2) until reaching 80%-90% confluence. MSCs were characterized as previously reported.[20] All experiments were performed with MSC cryopreserved between passages 3 and 4. For the in vivo experiments, we tested 2 donor samples, male and female, each of BM and UCT, and for the in vitro experiments, 3 donor samples (2 females and 1 male), each of BM and UCT were used.

Assessment of MSC Proliferation

To compare the proliferation of BM-MSC and UCT-MSC, cell growth curves were performed. In this assay, 1.0×10^5 cells were plated onto 100 mm × 25 mm cell culture dishes in standard expansion media (alpha MEM + 20% FBS). Cell culture dishes were harvested with TrypLE Select (Thermo Fisher Scientific, Waltham, MA) and counted at 24, 72, and 96 hours after cell plating. Manual cell counts with a hemocytometer were completed at each collection time point. 10× magnification photos (Olympus microscope, Pittsburgh, PA) were taken at each time point before cell harvest. In addition, cell proliferation was assessed at 48 hours by immunofluorescent staining with a rabbit monoclonal anti-Ki67 antibody (1:100; Abcam, Cambridge, MA), and DAPI (Vector Laboratories, Burlingame, CA). The proliferation index was determined by quantifying the Ki67-positive cells/total nucleated cells × 100. Cell viability was compared in UCT-MSC and BM-MSC by MTT assay (Sigma-Aldrich, Saint Louis, MO). MSC (1×10^4 cells/well) cultured in 96-well plates were exposed to normoxia (21% O2, 5% CO2) for 48 hours, followed by the addition of MTT labeling solution, according to the manufacturer's protocol. Absorbance was measured at a wavelength of 550 nm in a plate reader (Spectramax plus384 microplate reader; San Jose, CA). The

experiment was repeated with 3 batches of MSCs derived from different donors within each group. Graphpad Prism 9 was used to create the growth curves and graphs.

Assessment of BM and UCT-MSC Gene Expression

Inflammation and angiogenesis play a crucial role in BPD. MSCs have well-documented anti-inflammatory and pro-angiogenic properties. We, therefore, assessed the mRNA expression of the following anti-inflammatory genes known to be involved in BPD: IL-10 and TSG-6, along with the mRNA expression of the following pro-angiogenic genes: chemokine receptor 12 (CXCL12), vascular endothelial growth factor (VEGF), hepatocyte growth factor (HGF), angiopoietin-1 (Ang-1), and keratinocyte growth factor (KGF) using an ABI Fast 7500 System (Applied Bio-Rad, Foster City, CA) as previously described.[21] Briefly, total RNA isolated from UCT-MSC and BM-MSC were treated with DNase to remove possible DNA contamination. One microgram of total RNA was reverse-transcribed in a 20 µL reaction using a first-strand cDNA synthesis kit according to the manufacturer's protocol (Invitrogen, Grand Island, NY). Each reaction included diluted first-strand cDNA, specific primers, and master mix containing enzymes and TaqMan probes according to the manufacturer's instruction (Applied Biosystems). Real-time RT-PCR conditions were 95°C for 10 minutes, followed by 40 cycles of 95°C for 15 seconds and 60°C for 30 seconds. RNase-free water was used as a negative control. Primers for human IL-10, TSG-6, CXCL12, VEGF, HGF, Ang-1, KGF, and GAPDH were predeveloped by Applied Biosystems. For each target gene, a standard curve was established by performing a series of dilutions of the first-strand cDNA. The mRNA expression of target genes was normalized to GAPDH. Analyses were performed with 3 BM donor samples (2 females and 1 male) and 3 UCT donor samples (2 females and 1 male).

Wound Healing Assay

UCT-MSC and BM-MSC were cultured in Dulbecco's Modified Eagle Medium low glucose (Thermo Fisher Scientific, Waltham, MA) with 10% FBS as previously described.[22] The medium was exchanged with serum-free medium (SFM) with 20% knockout serum replacement (KOSR; Thermo Fisher Scientific, Waltham, MA). After a 72-hour incubation, the conditioned medium (CM) was collected. Confluent monolayers of human lung epithelial cells (A549; ATCC, Manassas, VA) cultured in F12K Medium, supplemented with 10% FBS were scored with a 200 µL yellow tip to leave a scratch. The culture medium was replaced with either (1) growth medium with KOSR SFM as control; or (2) growth medium with CM (× 2.0 concentration), based on pilot studies.

Wound closure was monitored by taking images at periodic time intervals after the scratch was performed. Images were captured with a light microscope (Leica DMI 6000, Buffalogrove, IL). The digitized images were then analyzed using TScratch program[23] to measure the open wound area at previously defined points. The wound closure rate was assessed by calculating the ratio of the open wound area after 24 and 48 hours to the open wound area at 0 hour, that is, the wound closure rate = (open area 0 hour – open area 24 hours or 48 hours)/open area 0 hour × 100%.

Matrigel Assay

The effect of UCT-MSC and BM-MSC CM on capillary tube formation of pulmonary microvascular endothelial cells (HULECs: ATCC, Manassas, VA) was determined by matrigel assay as previously described.[24] Briefly, HULECs, passage 3 to 4, were seeded at 2×10^4 cells/well into 96-well plates. Capillary tube formation was assessed on growth factor reduced matrigel-coated wells (BD Biosciences, San Diego, CA). Bright-field images were collected at 12 hours. All experiments were done in triplicate and tube formation was assessed using Image J Angiogenesis Analyzer.

Animals

The SYRCLE protocol for systemic review of animal intervention studies was adhered (Systemic Review Protocol for Animal Intervention Studies format by SYRCLE (www. SYRCLE.NL). Pregnant Sprague Dawley rats were purchased from Charles River Laboratories (Wilmington, MA). Animals were treated per National Institutes of Health guidelines. The protocol was approved by the Animal Care and Use Committee (ACUC) of the University of Miami Miller School of Medicine. The rats were randomly housed with food and water available ad libitum at constant temperature (25°C) under the 12:12 light/dark cycle.

Experimental Design

Sprague-Dawley newborn rats from 6 litters ($N = 60$) within 24 hours after birth were randomly selected and assigned to room air (RA) or hyperoxia (HYP) environments (85%-90% FiO$_2$) from postnatal day (P)1-P21, were given a single intra-tracheal (IT) injection of placebo (PL), BM-MSC or UCT-MSC on P3. Rats were housed in a plexiglass chamber with oxygen monitoring as previously described.[25,26] Oxygen exposure was continuous but briefly interrupted for animal care (<10 minutes/day). Nursing dams were rotated between normoxia and hyperoxia groups once every 48 hours to prevent oxygen toxicity to the dams. For IT injection, third passage MSC were thawed, assessed for viability, and washed with phosphate-buffered saline (PBS). MSCs were suspended in PBS at 1×10^6 viable cells per 50 µL for IT administration. This dose was chosen based on prior studies in our laboratory.[8] A single IT dose of 50 µL was administered to each pup. On P3, following sedation with isoflurane, the trachea was exposed through a small midline incision in the neck. MSC (1×10^6/50 µL) or PBS (PL) was delivered by direct tracheal puncture with a 30-gauge needle. Rats were placed in a warmed plastic chamber under normoxic or hyperoxic conditions for recovery. Once the rats were fully awake, they were returned to their dams. On P21, the rats were anesthetized with 1% isoflurane, tracheotomized and cannulated, and then sacrificed for analyses.

Lung Morphometric Analysis

Lung morphometry was performed as previously described.[27] Lungs were inflated and perfused with 4% paraformaldehyde (PFA) at a pressure of 15 cmH$_2$O for 5 minutes. The samples were left in PFA for 24 hours and serial dehydration in ethanol was performed the following day. The lungs were then embedded in paraffin. Serial 5-µm-thick paraffin-embedded sections obtained from the lung were stained with hematoxylin and eosin. Images from 10 randomly selected, nonoverlapping parenchymal fields were acquired from the lung sections of each animal at 10× magnification. Care was taken to exclude major bronchioles, vessels, and artifacts from the field. Images were captured by a blinded observer, and the mean linear intercept (MLI) and the radial-alveolar count (RAC), a measure of alveolarization were analyzed as previously described.[28]

Lung Angiogenesis

Vascular density was evaluated as previously described.[25] Briefly, lung sections were stained with polyclonal rabbit antihuman Von Willebrand Factor (vWF; 1:50; Dako, Carpinteria, CA), a marker of endothelial cells, and 4′6-di-amidino-2-phenylindole (DAPI; Vector Laboratories). Five randomly selected nonoverlapping parenchymal fields were evaluated from the lung sections of each animal. The number of blood vessels (20-50 μm in diameter) in each high-power field (HPF) was counted by a blinded observer.

Pulmonary Vascular Remodeling

Pulmonary vascular remodeling was evaluated as previously described.[27] Briefly, lung sections were stained with polyclonal rabbit antihuman vWF (1:50; Dako) and mouse anti-α-smooth muscle actin (α-SMA: 1:500, Sigma, St Louis, MO). Five randomly selected non-overlapping parenchymal fields were evaluated from the lung sections of each animal. Blood vessels (20-50 μm in diameter) in each HPF were counted by a blinded observer and the degree of muscularization was assessed.[28] Medial wall thickness was measured in 20 randomly selected arterioles (20-50 μm in diameter) at 40× magnification as previously described.[28] Briefly, the thickness of the medial layer of the arteriole was calculated using the formula 2× measured thickness of the medial layer/ average diameter of the vessel × 100%.

Assessment of Pulmonary Hypertension

Right ventricular systolic pressure (RVSP) was evaluated as a surrogate of pulmonary artery pressure. A thoracotomy was performed, and a 22-gauge needle connected to a pressure transducer was inserted into the right ventricle of P14 pups. RVSP was measured and recorded on a Gould polygraph (model TA-400; Gould Instruments, Cleveland, OH) as previously described.[28]

Assessment of Lung Inflammation

Lung macrophage infiltration was assessed by immunostaining lung sections with a rat monoclonal antibody to MAC-3 (1:20, BD Biosciences, San Jose, CA). The number of MAC-3 positive cells in the alveolar air spaces was determined by evaluating 10 random images taken with the 40× objective on each slide and quantifying the number of MAC-3-positive cells per HPF.[29]

Western Blot

Protein expression of the pro-inflammatory cytokine, monocyte chemoattractant protein (MCP-1) in homogenized lung samples was determined by Western Blot as previously described.[27] MCP-1 polyclonal antibody (1:500) was obtained from Abcam (Cambridge, MA). Briefly, lung homogenates were separated by 10% sodium dodecyl sulfate-polyacrylamide gel electrophoresis, transferred to nitrocellulose membranes, and blocked overnight at 4°C in 5% bovine serum albumin. Immunodetection was performed by incubating the membranes with the primary antibodies diluted in blocking buffer for 1 hour at room temperature. After washing, a semilumiscent horseradish peroxidase substrate was diluted in blocking buffer and applied for 60 minutes. Band intensity was quantified with the Quantity One software (Bio-Rad, Hercules, CA). β-Actin was used as the normalizing protein (1:10,000, Sigma-Aldrich).

Statistical Analysis

Data expressed as mean ± standard error of the mean (SEM) were analyzed by 2-way ANOVA with posthoc Holm-Sidak test using Sigma Stat software. *P* values less than .05 were considered statistically significant.

Results

Proliferative Capacity and Cell Morphology of BM-MSC and UCT-MSC

With clinical studies showing the promising therapeutic potential of MSC, it is crucial to obtain high yield and high-quality MSC. Hence, we compared UCT-MSC and BM-MSC viability by MTT assay and growth kinetics by cell proliferation assay and Ki67 immunostaining. MTT assay revealed that BM-MSC and UCT-MSC have similar cell viability (Fig. 1A). BM-MSC and UCT-MSC also showed a similar fibroblast-like (elongated spindle) morphology following 72 and 96 hours of cell culture (Fig. 1B), however, UCT-MSC showed a consistently higher growth rate. The difference was significant after 48 hours of cell culture (*P* < .05; Fig. 1C). Ki67 immunostaining also confirmed that UCT-MSC has a higher proliferation index than BM-MSC following 48 hours of cell culture (*P* < .05; Fig. 1D,E). Collectively, these data suggest that UCT-MSC proliferate at a greater rate as compared to BM-MSC.

Gene Expression Profile of BM-MSC and UCT-MSC

Given that BPD is a complex disease with aberrant lung inflammation and angiogenesis,[30] we next evaluated the expression of key anti-inflammatory and pro-angiogenic genes in BM-MSC and UCT-MSC. UCT-MSC had significantly higher gene expression of IL-10 (11-fold; *P* < .05) and TSG-6 (83-fold; *P* < .05) compared to BM-MSC (Fig. 2A,B), suggesting that UCT-MSC may possess greater anti-inflammatory effects compared to BM-MSC. Interestingly, BM-MSC had higher expression of CXCL12 (18-fold; *P* < .05) and VEGF (7-fold; *P* < .05) as compared to UCT-MSC (Fig. 2C,D). However, the expression of HGF and Ang-1, known angiogenic factors[31,32] that modulate lung angiogenesis, were higher in UCT-MSC as compared to the BM-MSCs (Fig. 2E,F). There was no difference in the expression of KGF, a known alveolar protective factor,[33] between the MSC sources.

Alveolar Protective and Wound Healing Effects of BM-MSC and UCT-MSC

BPD is characterized by an arrest of alveolar development. We, therefore, compared the effects of IT UCT-MSC and BM-MSC on lung alveolarization in an experimental BPD model. Newborn PL-treated hyperoxia-exposed rats exhibited severe destruction of the alveolar architecture, as evidenced by enlarged and simplified alveoli (Fig. 3A). Lung morphometric analysis demonstrated significantly decreased RAC and increased MLI in hyperoxia-exposed PL-treated rats (Fig. 3B,C). Administration of BM-MSC or UCT-MSC significantly increased RAC and while there was a trend for greater improvement with UCT-MSC, there was no significant difference between the HYP BM-MSC and HYP UCT-MSC groups (Fig. 3B). In addition, while both BM and UCT-MSC decreased the MLI, this was more marked in the UCT-MSC treated group (103 ± 4 vs 81 ± 3 vs 71 ± 3 μm;
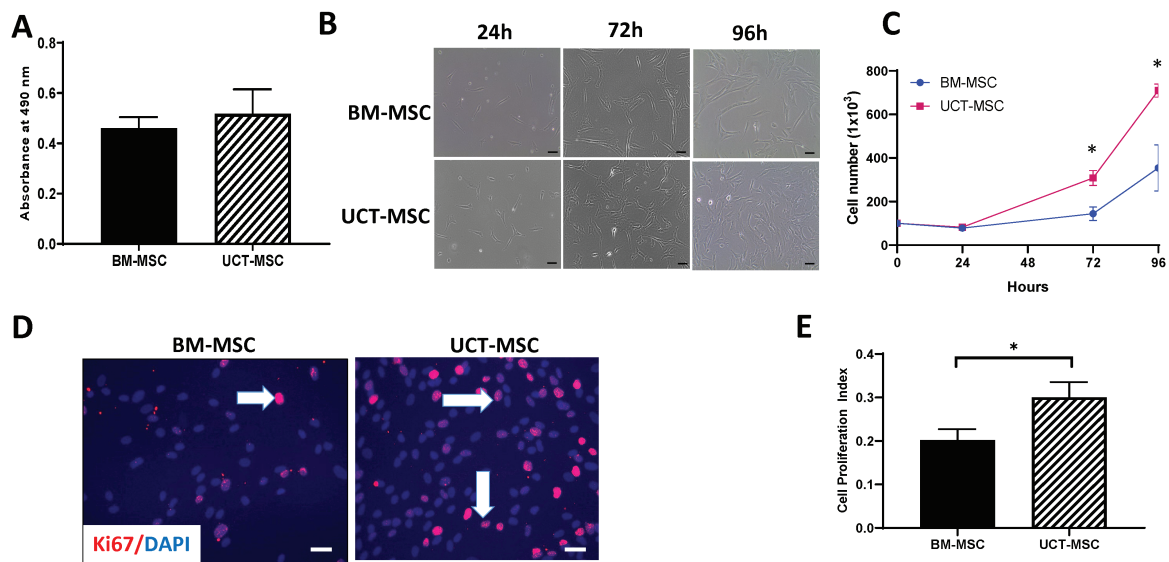
Figure 1. UCT-MSC have increased cell proliferation as compared to BM-MSC. (**A**) MTT assay showing similar cell viability of UCT-MSC and BM-MSC. (**B**) Morphology of cultured BM-MSC and UCT-MSC at 24, 72, and 96 hours. UCT-MSC and BM-MSC exhibited spindle-shaped morphology. Scale bars = 50 μm. Original magnification 10×. (**C**) Growth curves showing greater proliferation of UCT-MSC as compared to BM-MSC. (**D**) Representative microphotographs taken under 40X magnification showing increased Ki67-positive cells (red signal) in UCT-MSC compared to BM-MSC following 48 hours culture. (**E**) Quantification of the proliferation index (percentage of Ki67^{pos}nuclei/total nuclei) revealed that UCT-MSC had a higher proliferation index when compared to BM-MSC at 48 hours. All experiments were run in triplicates. Data are presented as mean ± SEM; *P < .05; N = 3 donors/group; BM-MSC versus UCT-MSC.
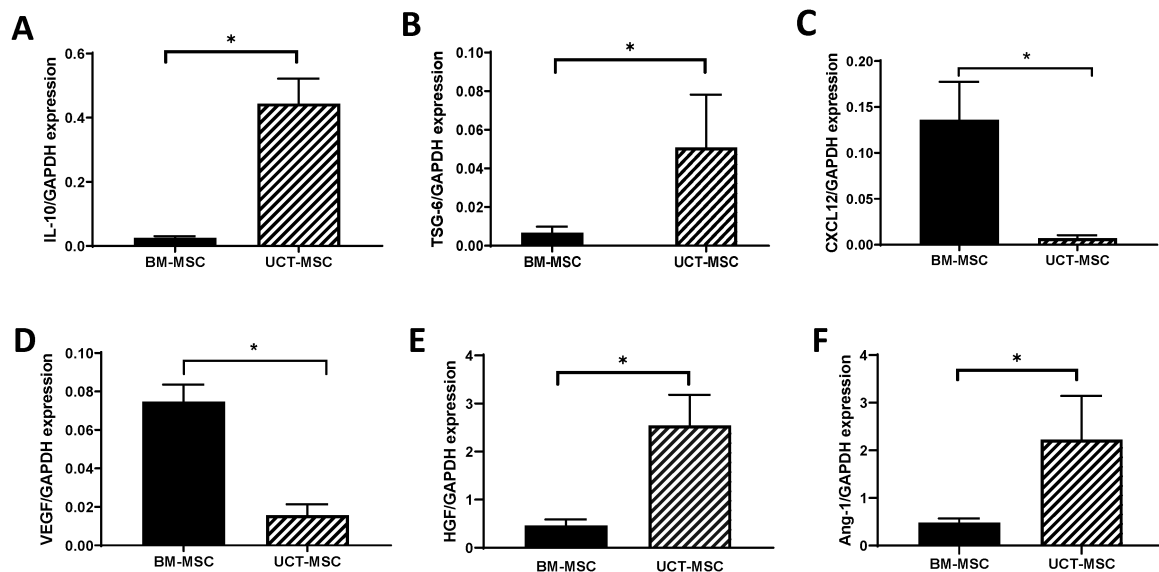

Figure 2. Comparison of BM-MSC and UCT-MSC anti-inflammatory and angiogenic gene profile. Increased expression of anti-inflammatory genes (**A**) IL-10 and (**B**) TSG-6 in UCT-MSC as compared to BM-MSC. BM-MSC has significantly increased (**C**) CXCL12 and (**D**) VEGF and decreased (**E**) HGF and (**F**) Ang-1 gene expression as compared to UCT-MSC. Data are presented as mean ± SEM; *P < .05; N = 3 donors/group; BM-MSC versus UCT-MSC.

HYP-PL vs HYP BM-MSC vs HYP UCT-MSC; P < .05, N = 8-10/group) (Fig. 3C). Immunostaining of lung sections with Ki67 and cleaved caspase-3 antibodies revealed that there was no difference in lung cell proliferation or apoptosis between the MSC treatment groups (data not shown).

Given the known paracrine-mediated effects of MSCs, we also sought to ascertain whether UCT and BM-MSC CM would have differential effects on lung epithelial cell wound healing. Scratch-injured human lung epithelial cells were incubated in CM from UCT-MSC and BM-MSC and wound closure was assessed at 0, 24, and 48 hours, respectively.

Scratch width was not significantly different between the groups at 0 and 24 hours (Fig. 3D,E). In contrast, at 48 hours, lung epithelial cells exposed to UCT-MSC CM had significantly greater wound closure as compared to BM-MSC CM (Fig. 3D,E).

Effects of BM-MSC and UCT-MSC on Lung Angiogenesis

Disordered angiogenesis is a key feature of BPD. Thus, we next compared the effect of UCT-MSC and BM-MSC in preserving lung angiogenesis in our experimental BPD model.
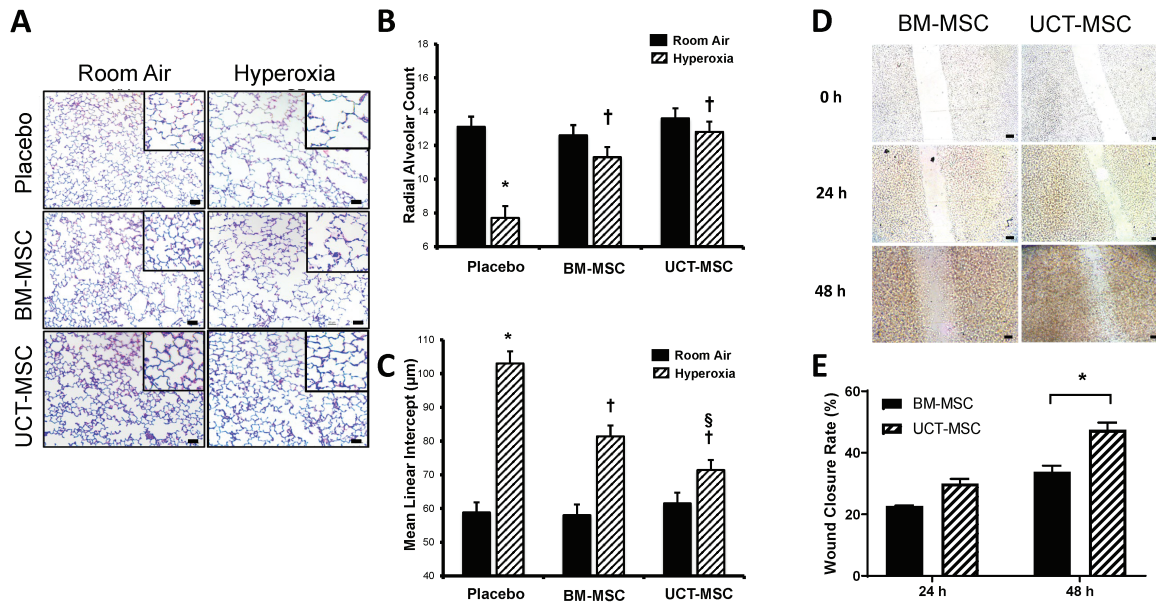
Figure 3. Effects of BM-MSC and UCT-MSC on lung alveolarization and wound healing. (**A**) Hematoxylin and eosin-stained lung sections demonstrating improved alveolar structure in hyperoxia-exposed rats treated with BM-MSC or UCT-MSC. Original magnification 100×. Scale bars = 50 μm. Morphometric analysis showed significantly (**B**) increased radial alveolar count (RAC) and (**C**) decreased mean linear intercept (MLI) in both hyperoxia UCT-MSC and BM-MSC-treated groups. However, the decrease in MLI was most marked in UCT-MSC-treated group. Data are presented as mean ± SEM; *$P < .05$; RA-PL vs hyperoxia-PL; †$P < .05$, hyperoxia-PL versus hyperoxia BM-MSC or hyperoxia UCT-MSC; § $P < .05$, hyperoxia BM-MSC vs hyperoxia UCT-MSC, $N = 8$-10/group. (**D**) Representative time-lapse images of lung epithelial cells incubated in serum free UCT-MSC conditioned media (CM) or BM-MSC CM immediately after the scratches and at 24 and 48 hours. Scale bars = 200 μm. Original magnification 100×. (**E**) There was a significant increase in the extent of wound closure in lung epithelial cells exposed to UCT-MSC CM compared to BM-MSC CM at 48 hours. All experiments were run in triplicates. Data are presented as mean ± SEM; *$P < .05$, BM-MSC versus UCT-MSC, $N = 3$ donors/group.
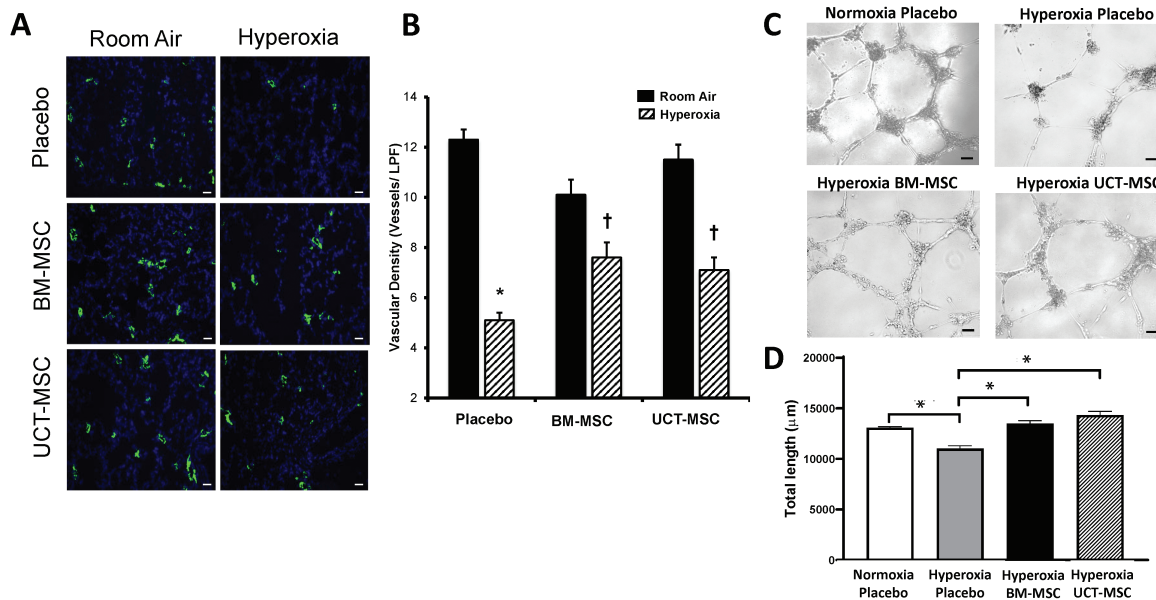

Figure 4. BM-MSC and UCT-MSC similarly improve lung angiogenesis and promote capillary tube formation. (**A**) Representative lung sections stained with Von Willebrand Factor (green) and 4′6-diamidino-2-phenylindole (DAPI: blue) showing increased vessels in both MSC groups. Original magnification 100×. Scale bars = 50 μm. (**B**) Similar improvement in lung vascular density in both UCT-MSC and BM-MSC hyperoxia-exposed groups. Data are presented as mean ± SEM; *$P < .05$, RA-PL versus hyperoxia-PL; † $P < .05$, hyperoxia-PL vs hyperoxia BM-MSC or hyperoxia UCT-MSC, $N = 8$-10/group. (**C**) BM-MSC CM and UCT-MSC CM similarly promote capillary tube formation in hyperoxia-exposed pulmonary microvascular endothelial cells (HULEC). All experiments were run in triplicates. Data are presented as mean ± SEM; *$P < .05$, BM-MSC versus UCT-MSC, $N = 3$ donors/group.

Angiogenesis was determined by staining lung sections with vWF antibody (Fig. 4A). There was no difference in vascular density between the RA groups. As compared to RA-PL, hyperoxia-exposed rats had significantly decreased vascular density. In contrast, administration of BM-MSC or UCT-MSC to hyperoxia-exposed rats improved angiogenesis (5 ± 0.4 vs 7 ± 0.6 vs 7 ± 0.6 vessels per HPF; HYP-PL vs HYP BM-MSC vs HYP UCT-MSC; $P < .05$, $N = 8$-10/group) (Fig. 4A,B).

There was however no difference between the hyperoxia MSC-treated groups.

Moreover, HULECs exposed to normoxic or hyperoxic conditions were also incubated with BM-MSC CM, UCT-MSC CM, or control for 24 hours. Matrigel assay revealed that whereas hyperoxia control HULECs had decreased capillary tube formation, both BM-MSC CM and UCT-MSC CM significantly promoted capillary tube formation and there was no difference between the treatment groups (Fig. 4C,D).

Effect of BM-MSC and UCT-MSC on Pulmonary Hypertension and Vascular Remodeling

Pulmonary vascular remodeling was determined by quantifying the medial wall thickness and percentage of muscularized vessels. As compared to RA-PL, exposure to hyperoxia significantly increased medial wall thickness and percentage of muscularized vessels (Fig. 5A-C). Treatment with UCT-MSC or BM-MSC significantly reduced medial wall thickness and percentage of muscularized vessels and there was no difference between the group (Fig. 5A-C). Additionally, whereas hyperoxia-exposed PL treated rats had increased RVSP (20 ± 0.8 vs $40 \pm 3\%$, RA-PL vs HYP-PL; $P < 0.05$, $N = 8$-10/group), administration of BM-MSC and UCT-MSC decreased RVSP (40 ± 3 vs 35 ± 2 vs 32 ± 2 mm Hg; HYP-PL vs HYP BM-MSC vs HYP UCT-MSC; $P < .05$, $N = 8$-10/group). There was no difference between the MSC-treatment groups. Taken together, these findings demonstrate that UCT-MSC and BM-MSC reduce pulmonary hypertension and vascular remodeling in experimental BPD, and this is not influenced by the MSC source.

Effect of BM-MSC and UCT-MSC on Lung Inflammation

There was no difference in lung macrophage infiltration in RA-exposed rats. In contrast, hyperoxia-exposed PL-treated rats had a 4-fold increase in the number of the MAC-3 positive cells per HPF. Administration of UCT-MSC and BM-MSC significantly reduced lung macrophage infiltration in hyperoxia-exposed rats but this was most significant in the UCT-MSC group (Fig. 6A,B). In addition, Western Blot analysis demonstrated that hyperoxia exposure significantly increased MCP-1 expression in lung lysates and this was significantly reduced by UCT-MSC and BM-MSC. The reduction was most pronounced in the hyperoxia-exposed UCT-MSC group (Fig. 6C). UCT-MSC and BM-MSC also significantly reduced lung IL-1β, or TNF-α gene expression in hyperoxia-exposed rats but there was no difference in their expression between the hyperoxia MSC-groups (Fig. 6D,E).

Discussion

Early clinical trials investigating MSC therapy in newborns with BPD show that they are safe and have potential beneficial effects.[34] However, a lack of consensus on the ideal source of MSC to treat BPD still exists. Understanding the role of many variables involved in successful MSC therapy, including the ideal source of MSC for BPD therapy, will contribute to the optimization of MSC in future clinical trials. Herein, we performed a comparative analysis of the lung-protective effects of UCT-MSC and BM-MSC in an experimental model of BPD. UCT and BM-MSC were administered during the newborn period to rodents with hyperoxia-induced lung
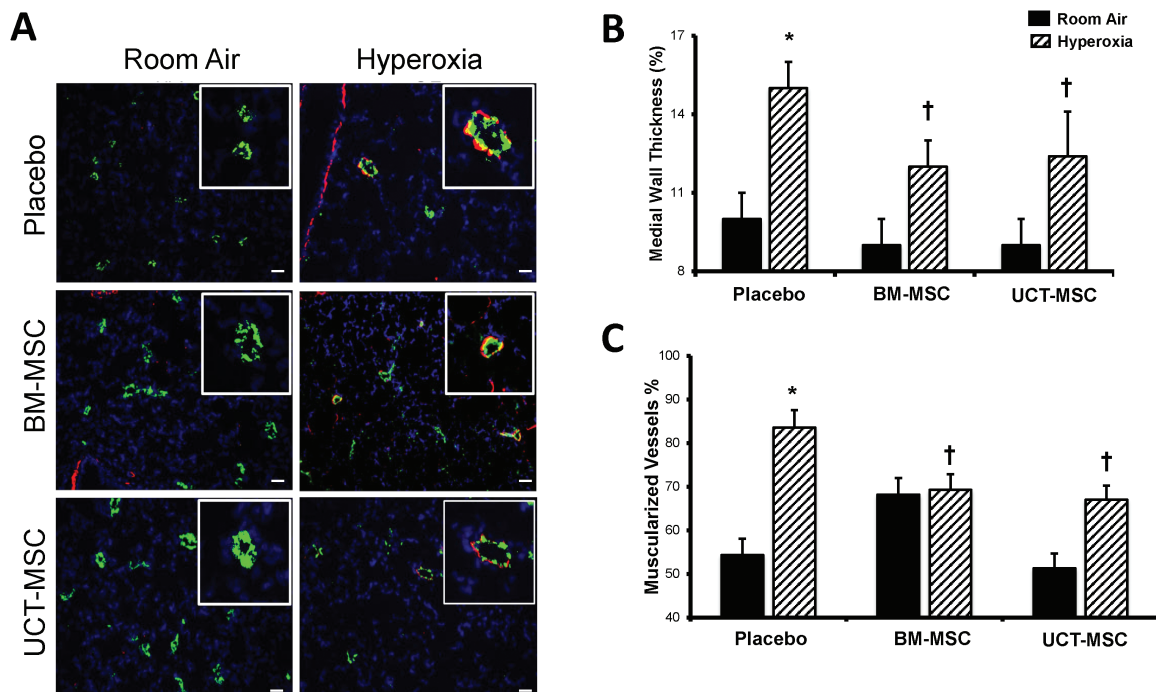

Figure 5. BM-MSC and UCT-MSC similarly improve pulmonary vascular remodeling. (**A**) Lung sections stained with Von Willebrand Factor (green), α-smooth muscle actin (red), and DAPI (blue), demonstrating improved vascular remodeling in hyperoxia-exposed rats treated with BM-MSC or UCT-MSC. Original magnification 100×. Scale bars=50 µm. Compared with the hyperoxia-PL group, (**B**) medial wall thickness (MWT) and (**C**) percentage of muscularized vessels were reduced in hyperoxia-exposed MSC-treated group. Data are presented as mean ± SEM; *P < .05, RA-PL versus hyperoxia-PL; † *P* < .05, hyperoxia-PL versus hyperoxia BM-MSC or hyperoxia UCT-MSC, *N* = 8-10/group.
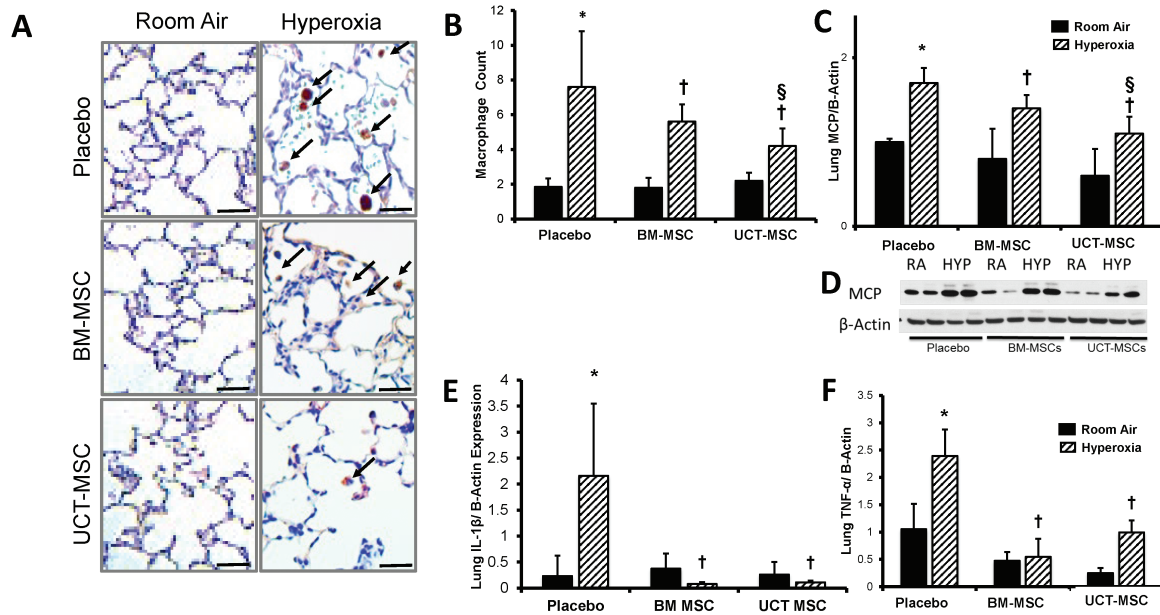
Figure 6. Effect of BM-MSC and UCT-MSC on lung inflammation. (**A**) Representative lung sections immunostained with Mac-3 (macrophage marker, brown signal) showing reduced macrophage infiltration in hyperoxia-exposed rats treated with BM-MSC or UCT-MSC. (**B**) Bar graph showing significantly decreased number of macrophages per high power field in hyperoxia-exposed BM-MSC or UCT-MSC groups. The reduction was most pronounced in the UCT-MSC treated group. (**C**) Significantly decreased lung MCP-1 expression in hyperoxic rats treated with UCT-MSC and BM-MSC, but this was most marked in the UCT-MSC group. (**D**) Representative Western blot of MCP-1 is shown. β-actin is utilized as the normalized protein. Reduced (**E**) IL-1β and (**F**) TNF-α expression in both UCT-MSC and BM-MSC hyperoxia-exposed groups. Data are presented as mean ± SEM; *$P < .05$, RA-PL versus hyperoxia-PL; † $P < .05$, hyperoxia-PL versus hyperoxia BM-MSC or hyperoxia UCT-MSC; § $P < .05$, hyperoxia BM-MSC versus hyperoxia UCT-MSC, N = 6-8/group.

injury and structural and functional markers of lung repair were analyzed at 3 weeks. We demonstrate that UCT-MSC and BM-MSC have similar effects on lung angiogenesis and vascular remodeling however UCT-MSC suppresses lung macrophage infiltration and promotes lung epithelial cell wound healing to a greater degree than BM-MSC. There were also trends for better alveolar protection in the animals that received UCT-MSC. These findings have significant implications as cell therapy for BPD moves from the bench to the bedside.

Inflammation is a key contributor to aberrant lung development and remodeling in preterm infants with BPD.[25] Prior studies have demonstrated that MSC from UCB, UCT, and BM attenuate lung injury in experimental BPD models by decreasing inflammation,[2,11] but the evidence was heretofore lacking on their comparative efficacy. MSC attenuate the respiratory burst in activated neutrophils,[35] suppress natural killer cell proliferation, cytokine production, and cytotoxicity,[36] inhibit dendritic cell maturation, and activation,[37] induce changes in macrophage polarization to an M2, anti-inflammatory phenotype,[38-40] suppress T-cell cytokine secretion and cytotoxicity[41-43] and inhibit B-cell survival, proliferation, and differentiation.[44] UCT-MSC may have superior immunomodulatory properties as compared to BM-MSC but published findings are inconsistent.[13,16] Our present in vivo studies show that UCT-MSC and BM-MSC treated hyperoxia-exposed rats have a similar reduction in lung IL-1β and TNF-α gene expression but interestingly hyperoxia-exposed rats who received UCT-MSC had significantly lower lung macrophage infiltration than rats that received BM-MSC. MCP-1, a key chemokine involved in macrophage infiltration and BPD pathogenesis were also significantly lower in hyperoxia-exposed rats that received

UCT-MSC.[45] In keeping with these in vivo findings, our in vitro studies also revealed that UCT-MSC has a higher expression of the anti-inflammatory cytokines, IL-10 and TSG-6 as compared to BM-MSC. Interestingly, BM-MSC has variable TSG-6 expression, and cells with higher TSG-6 levels have better regenerative effects.[46] TSG-6 knockdown attenuates the anti-inflammatory and regenerative effects of MSC in neonatal hyperoxia-induced lung injury.[47] Additionally, we previously demonstrated that IT administration of an adenovirus over-expressing TSG-6 attenuates neonatal hyperoxia-induced lung injury and lung macrophage infiltration.[25] Taken together, our findings suggest that UCT and BM-MSC have significant lung anti-inflammatory effects but UCT-MSC suppress lung macrophage infiltration to a greater degree in our experimental BPD model.

Another important finding in our current study was our in vitro scratch assay showing superior effects of UCT-MSC CM on lung epithelial cell wound healing. Our laboratory previously demonstrated that the regenerative effects of MSC are mainly paracrine mediated[4] and other investigators have demonstrated that BM-MSC and UCT-MSC enhance cell proliferation and migration, leading to improved wound repair.[48,49] No comparative analyses have however been performed. Interestingly, in our in vivo experimental BPD model, UCT-MSC and BM-MSC had similar effects on lung cell proliferation and apoptosis, but hyperoxia-exposed rats that received UCT-MSC had trends for better alveolar protection as compared to those that received BM-MSC. We postulate that these potential superior benefits on alveolarization by UCT-MSCs are in part secondary to its greater effects on cell migration, as seen in our wound healing assay. Moreover, in keeping with this finding, our in vitro study also showed that

UCT-MSC exhibit greater HGF expression, a critical factor in cell migration and wound repair.[50]

Poor lung vascular growth is also a major finding in BPD. In rodent models of BPD, MSC regenerative effects are in part mediated by vascular endothelial growth factor (VEGF)[51] and CXCL12.[6] There is also evidence that other growth factors such as Ang-1, KGF, and HGF restore endothelial cell integrity.[52-57] Intriguingly, our in vitro studies revealed that BM-MSC has greater VEGF and CXCL12 expression. Despite this, in our experimental BPD model, BM-MSC and UCT-MSC treated hyperoxia-exposed rats had similar improvements on lung vascular density, pulmonary vascular remodeling, and pulmonary hypertension. Additionally, in our in vitro angiogenesis assay, UCT-MSC CM and BM-MSC CM had similar effects on capillary tube formation. We postulate that our current finding of similar beneficial effects on lung angiogenesis in our experimental BPD model with both MSC sources, despite higher VEGF and CXCL12 expression in BM-MSC may be in part secondary to greater HGF and Ang-1 expression in UCT-MSC.

Our study has specific strengths and limitations. First, consistent with previous studies, our in-vitro study shows that the growth kinetics of the UCT-MSC was significantly higher than BM-MSC. Greater proliferation allows for shorter cell culture time to generate a sufficient population of MSC for clinical use. It should however be recognized that although we investigated MSC from 6 different donors ($N = 3$/MSC source), small variations in the source and processing methods may change the functional properties of the final MSC product. Even the most rigorously sorted stem cell population might be heterogeneous. Previous large sample analyses from UCT-MSC have however revealed consistent properties among the donors.[58] For our in vivo studies, we also used freshly thawed cells, but studies comparing the efficacy of thawed and culture-rescued MSC products have yielded mixed results.[59] We however previously showed significant therapeutic efficacy using freshly thawed cells.[8] Another factor to consider is that it is possible that the superior effects of UCT-MSC on lung macrophage infiltration and wound healing may be secondary to the age of the donor and not per se the source of the cells. This age-dependent beneficial effect of MSC is crucial as there is strong evidence that MSC from young donors promotes more rapid and robust wound repair compared to old MSC.[58,60,61] Our preclinical hyperoxia BPD model is also imperfect as BPD is multifactorial. Moving forward, further studies in large animal models will be important.

Conclusion

To the best of our knowledge, this is the first published report comparing the efficacy of BM-MSC and UCT-MSC in an experimental BPD model. We show that BM-MSC and UCT-MSC have potent lung regenerative effects, but UCT-MSC has potentially better alveolar protective effects, suppresses lung macrophage infiltration, and promotes epithelial cell wound healing to a greater degree as compared to BM-MSC. Given that UCT-MSC is readily accessible,[62] less likely to have karyotype abnormalities[63] and more easy to isolate and culture,[64] with minimal ethical concerns, these findings have fundamentally important implications for MSC therapy in BPD prevention.

Conflict of Interest

J.M.H. declared patent holder, stock ownership, and advisory role for Longeveron and Heart Genomics; Research funding from NHLBI. The other authors indicated no potential conflicts of interest.

Author Contributions

M.B., B.C.: collection and/or assembly of data, data analysis and interpretation, manuscript writing, and final approval of the manuscript; S.S., M.S., P.C., J.D.: collection and/or assembly of data, data analysis and interpretation, and final approval of the manuscript; K.V., M.A.B.: provision of study material or patients and final approval of the manuscript; A.D., J.H., R.Z., A.S., S.W.: collection and/or assembly of data and final approval of the manuscript; O.C.V., J.M.H.: conception and design and final approval of the manuscript; A.K.: conception and design, provision of study material or patients, and final approval of the manuscript; K.C.Y.: conception and design, collection and/or assembly of data, data analysis and interpretation, financial Support, and final approval of the manuscript.

Data Availability

The data that support the findings of this study are available from the corresponding author upon reasonable request.

References

1. Higgins RD, Jobe AH, Koso-Thomas M, et al. Bronchopulmonary dysplasia: executive summary of a workshop. *J Pediatr.* 2018;197:300-308.
2. Aslam M, Baveja R, Liang OD, et al. Bone marrow stromal cells attenuate lung injury in a murine model of neonatal chronic lung disease. *Am J Respir Crit Care Med.* 2009;180(11):1122-1130.
3. Andrzejewska A, Lukomska B, Janowski M. Concise review: mesenchymal stem cells: from roots to boost. *Stem Cells.* 2019;37(7):855-864.
4. Sutsko RP, Young KC, Ribeiro A, et al. Long-term reparative effects of mesenchymal stem cell therapy following neonatal hyperoxia-induced lung injury. *Pediatr Res.* 2013;73(1):46-53.
5. van Haaften T, Byrne R, Bonnet S, et al. Airway delivery of mesenchymal stem cells prevents arrested alveolar growth in neonatal lung injury in rats. *Am J Respir Crit Care Med.* 2009;180(11):1131-1142.
6. Reiter J, Drummond S, Sammour I, et al. Stromal derived factor-1 mediates the lung regenerative effects of mesenchymal stem cells in a rodent model of bronchopulmonary dysplasia. *Respir Res.* 2017;18(1):137.
7. Tropea KA, Leder E, Aslam M, et al. Bronchioalveolar stem cells increase after mesenchymal stromal cell treatment in a mouse model of bronchopulmonary dysplasia. *Am J Physiol Lung Cell Mol Physiol.* 2012;302(9):L829-L837.

8. Sammour I, Somashekar S, Huang J, et al. The effect of gender on mesenchymal stem cell (MSC) efficacy in neonatal hyperoxia-induced lung injury. *PLoS One*. 2016;11(10):e0164269.

9. Sung DK, Chang YS, Ahn SY, et al. Optimal route for human umbilical cord blood-derived mesenchymal stem cell transplantation to protect against neonatal Hyperoxic lung injury: gene expression profiles and histopathology. *PLoS One*. 2015;10(8):e0135574.

10. Chang YS, Choi SJ, Ahn SY, et al. Timing of umbilical cord blood derived mesenchymal stem cells transplantation determines therapeutic efficacy in the neonatal hyperoxic lung injury. *PLoS One*. 2013;8(1):e52419.

11. Chang YS, Oh W, Choi SJ, et al. Human umbilical cord blood-derived mesenchymal stem cells attenuate hyperoxia-induced lung injury in neonatal rats. *Cell Transplant*. 2009;18(8):869-886.

12. Kern S, Eichler H, Stoeve J, Klüter H, Bieback K. Comparative analysis of mesenchymal stem cells from bone marrow, umbilical cord blood, or adipose tissue. *Stem Cells*. 2006;24(5):1294-1301.

13. Bárcia RN, Santos JM, Filipe M, et al. What makes umbilical cord tissue-derived mesenchymal stromal cells superior immunomodulators when compared to bone marrow derived mesenchymal stromal cells? *Stem Cells Int*. 2015;2015:583984.

14. Javed MJ, Mead LE, Prater D, et al. Endothelial colony forming cells and mesenchymal stem cells are enriched at different gestational ages in human umbilical cord blood. *Pediatr Res*. 2008;64(1):68-73.

15. Secunda R, Vennila R, Mohanashankar AM, Rajasundari M, Jeswanth S, Surendran R. Isolation, expansion and characterisation of mesenchymal stem cells from human bone marrow, adipose tissue, umbilical cord blood and matrix: a comparative study. *Cytotechnology*. 2015;67(5):793-807.

16. Vieira Paladino F, de Moraes Rodrigues J, da Silva A, Goldberg AC. The immunomodulatory potential of wharton's jelly mesenchymal stem/stromal cells. *Stem Cells Int*. 2019;2019:3548917.

17. Weiss ML, Anderson C, Medicetty S, et al. Immune properties of human umbilical cord Wharton's jelly-derived cells. *Stem Cells*. 2008;26(11):2865-2874.

18. Chen MY, Lie PC, Li ZL, Wei X. Endothelial differentiation of Wharton's jelly-derived mesenchymal stem cells in comparison with bone marrow-derived mesenchymal stem cells. *Exp Hematol*. 2009;37(5):629-640.

19. Li X, Bai J, Ji X, Li R, Xuan Y, Wang Y. Comprehensive characterization of four different populations of human mesenchymal stem cells as regards their immune properties, proliferation and differentiation. *Int J Mol Med*. 2014;34(3):695-704.

20. Karaoz E, Aksoy A, Ayhan S, Sariboyaci AE, Kaymaz F, Kasap M. Characterization of mesenchymal stem cells from rat bone marrow: ultrastructural properties, differentiation potential and immunophenotypic markers. *Histochem Cell Biol*. 2009;132(5):533-546.

21. Shafieian M, Chen S, Wu S. Integrin-linked kinase mediates CTGF-induced epithelial to mesenchymal transition in alveolar type II epithelial cells. *Pediatr Res*. 2015;77(4):520-527.

22. Walter MN, Wright KT, Fuller HR, MacNeil S, Johnson WE. Mesenchymal stem cell-conditioned medium accelerates skin wound healing: an in vitro study of fibroblast and keratinocyte scratch assays. *Exp Cell Res*. 2010;316(7):1271-1281.

23. Gebäck T, Schulz MM, Koumoutsakos P, Detmar M. TScratch: a novel and simple software tool for automated analysis of monolayer wound healing assays. *Biotechniques*. 2009;46(4):265-274.

24. Arnaoutova I, Kleinman HK. In vitro angiogenesis: endothelial cell tube formation on gelled basement membrane extract. *Nat Protoc*. 2010;5(4):628-635.

25. Bryan C, Sammour I, Guerra K, et al. TNFα-stimulated protein 6 (TSG-6) reduces lung inflammation in an experimental model of bronchopulmonary dysplasia. *Pediatr Res*. 2019;85(3):390-397.

26. Benny M, Hernandez DR, Sharma M, et al. Neonatal hyperoxia exposure induces aortic biomechanical alterations and cardiac dysfunction in juvenile rats. *Physiol Rep*. 2020;8(1):e14334.

27. Chen S, Rong M, Platteau A, et al. CTGF disrupts alveolarization and induces pulmonary hypertension in neonatal mice: implication in the pathogenesis of severe bronchopulmonary dysplasia. *Am J Physiol Lung Cell Mol Physiol*. 2011;300(3):L330-L340.

28. Young KC, Torres E, Hatzistergos KE, Hehre D, Suguihara C, Hare JM. Inhibition of the SDF-1/CXCR4 axis attenuates neonatal hypoxia-induced pulmonary hypertension. *Circ Res*. 2009;104(11):1293-1301.

29. Dapaah-Siakwan F, Zambrano R, Luo S, et al. Caspase-1 inhibition attenuates hyperoxia-induced lung and brain injury in neonatal mice. *Am J Respir Cell Mol Biol*. 2019;61(3):341-354.

30. Baker CD, Abman SH. Impaired pulmonary vascular development in bronchopulmonary dysplasia. *Neonatology*. 2015;107(4):344-351.

31. Seedorf G, Metoxen AJ, Rock R, et al. Hepatocyte growth factor as a downstream mediator of vascular endothelial growth factor-dependent preservation of growth in the developing lung. *Am J Physiol Lung Cell Mol Physiol*. 2016;310(11):L1098-L1110.

32. Syed M, Das P, Pawar A, et al. Hyperoxia causes miR-34a-mediated injury via angiopoietin-1 in neonatal lungs. *Nat Commun*. 2017;8(1):1173.

33. Franco-Montoya ML, Bourbon JR, Durrmeyer X, Lorotte S, Jarreau PH, Delacourt C. Pulmonary effects of keratinocyte growth factor in newborn rats exposed to hyperoxia. *Am J Physiol Lung Cell Mol Physiol*. 2009;297(5):L965-L976.

34. Ahn SY, Chang YS, Kim JH, Sung SI, Park WS. Two-year follow-up outcomes of premature infants enrolled in the phase i trial of mesenchymal stem cells transplantation for bronchopulmonary dysplasia. *J Pediatr*. 2017;185:49-54.e2.

35. Raffaghello L, Bianchi G, Bertolotto M, et al. Human mesenchymal stem cells inhibit neutrophil apoptosis: a model for neutrophil preservation in the bone marrow niche. *Stem Cells*. 2008;26(1):151-162.

36. Sotiropoulou PA, Perez SA, Gritzapis AD, Baxevanis CN, Papamichail M. Interactions between human mesenchymal stem cells and natural killer cells. *Stem Cells*. 2006;24(1):74-85.

37. Nauta AJ, Kruisselbrink AB, Lurvink E, Willemze R, Fibbe WE. Mesenchymal stem cells inhibit generation and function of both CD34+-derived and monocyte-derived dendritic cells. *J Immunol*. 2006;177(4):2080-2087.

38. Ko JH, Lee HJ, Jeong HJ, et al. Mesenchymal stem/stromal cells precondition lung monocytes/macrophages to produce tolerance against allo- and autoimmunity in the eye. *Proc Natl Acad Sci USA*. 2016;113(1):158-163.

39. Németh K, Leelahavanichkul A, Yuen PS, et al. Bone marrow stromal cells attenuate sepsis via prostaglandin E(2)-dependent reprogramming of host macrophages to increase their interleukin-10 production. *Nat Med*. 2009;15(1):42-49.

40. Kim J, Hematti P. Mesenchymal stem cell-educated macrophages: a novel type of alternatively activated macrophages. *Exp Hematol*. 2009;37(12):1445-1453.

41. Meisel R, Zibert A, Laryea M, Göbel U, Däubener W, Dilloo D. Human bone marrow stromal cells inhibit allogeneic T-cell responses by indoleamine 2,3-dioxygenase-mediated tryptophan degradation. *Blood*. 2004;103(12):4619-4621.

42. Zappia E, Casazza S, Pedemonte E, et al. Mesenchymal stem cells ameliorate experimental autoimmune encephalomyelitis inducing T-cell anergy. *Blood*. 2005;106(5):1755-1761.

43. Krampera M, Glennie S, Dyson J, et al. Bone marrow mesenchymal stem cells inhibit the response of naive and memory antigen-specific T cells to their cognate peptide. *Blood*. 2003;101(9):3722-3729.

44. Corcione A, Benvenuto F, Ferretti E, et al. Human mesenchymal stem cells modulate B-cell functions. *Blood*. 2006;107(1):367-372.

45. Vozzelli MA, Mason SN, Whorton MH, Auten RL Jr. Antimacrophage chemokine treatment prevents neutrophil and macrophage influx in hyperoxia-exposed newborn rat lung. *Am J Physiol Lung Cell Mol Physiol*. 2004;286(3):L488-L493.

46. Oh JY, Roddy GW, Choi H, et al. Anti-inflammatory protein TSG-6 reduces inflammatory damage to the cornea following chemical and

mechanical injury. *Proc Natl Acad Sci U S A*. 2010;107(39):16875-16880.

47. Chaubey S, Thueson S, Ponnalagu D, et al. Early gestational mesenchymal stem cell secretome attenuates experimental bronchopulmonary dysplasia in part via exosome-associated factor TSG-6. *Stem Cell Res Ther*. 2018;9(1):173.

48. Hocking AM, Gibran NS. Mesenchymal stem cells: paracrine signaling and differentiation during cutaneous wound repair. *Exp Cell Res*. 2010;316(14):2213-2219.

49. Arno AI, Amini-Nik S, Blit PH, et al. Human Wharton's jelly mesenchymal stem cells promote skin wound healing through paracrine signaling. *Stem Cell Res Ther*. 2014;5(1):28.

50. Ito Y, Correll K, Schiel JA, Finigan JH, Prekeris R, Mason RJ. Lung fibroblasts accelerate wound closure in human alveolar epithelial cells through hepatocyte growth factor/c-Met signaling. *Am J Physiol Lung Cell Mol Physiol*. 2014;307(1):L94-105.

51. Chang YS, Ahn SY, Jeon HB, et al. Critical role of vascular endothelial growth factor secreted by mesenchymal stem cells in hyperoxic lung injury. *Am J Respir Cell Mol Biol*. 2014;51(3):391-399.

52. Fang X, Neyrinck AP, Matthay MA, Lee JW. Allogeneic human mesenchymal stem cells restore epithelial protein permeability in cultured human alveolar type II cells by secretion of angiopoietin-1. *J Biol Chem*. 2010;285(34):26211-26222.

53. Zhao YD, Ohkawara H, Vogel SM, Malik AB, Zhao YY. Bone marrow-derived progenitor cells prevent thrombin-induced increase in lung vascular permeability. *Am J Physiol Lung Cell Mol Physiol*. 2010;298(1):L36-L44.

54. Lee JW, Fang X, Gupta N, Serikov V, Matthay MA. Allogeneic human mesenchymal stem cells for treatment of *E. coli* endotoxin-induced acute lung injury in the ex vivo perfused human lung. *Proc Natl Acad Sci USA*. 2009;106(38):16357-16362.

55. Mei SHJ, McCarter SD, Deng Y, Parker CH, Liles WC, Stewart DJ. Prevention of LPS-induced acute lung injury in Mice by mesenchymal stem cells overexpressing angiopoietin 1. *PLoS Med*. 2007;4:e269.

56. Katsha AM, Ohkouchi S, Xin H, et al. Paracrine factors of multipotent stromal cells ameliorate lung injury in an elastase-induced emphysema model. *Mol Ther*. 2011;19(1):196-203.

57. Lee JW, Fang X, Krasnodembskaya A, Howard JP, Matthay MA. Concise review: Mesenchymal stem cells for acute lung injury: role of paracrine soluble factors. *Stem Cells*. 2011;29(6):913-919.

58. Raileanu VN, Whiteley J, Chow T, et al. Banking mesenchymal stromal cells from umbilical cord tissue: large sample size analysis reveals consistency between donors. *Stem Cells Transl Med*. 2019;8(10):1041-1054.

59. Tan Y, Salkhordeh M, Wang JP, et al. Thawed mesenchymal stem cell product shows comparable immunomodulatory potency to cultured cells in vitro and in polymicrobial septic animals. *Sci Rep*. 2019;9(1):18078.

60. Khong SML, Lee M, Kosaric N, et al. Single-cell transcriptomics of human Mesenchymal stem cells reveal age-related cellular subpopulation depletion and impaired regenerative function. *Stem Cells*. 2019;37(2):240-246.

61. Wiese DM, Ruttan CC, Wood CA, Ford BN, Braid LR. Accumulating transcriptome drift precedes cell aging in human umbilical cord-derived mesenchymal stromal cells serially cultured to Replicative senescence. *Stem Cells Transl Med*. 2019;8(9):945-958.

62. Malgieri A, Kantzari E, Patrizi MP, Gambardella S. Bone marrow and umbilical cord blood human mesenchymal stem cells: state of the art. *Int J Clin Exp Med*. 2010;3(4):248-269.

63. Ruan ZB, Zhu L, Yin YG, Chen GC. Karyotype stability of human umbilical cord-derived mesenchymal stem cells during in vitro culture. *Exp Ther Med*. 2014;8(5):1508-1512.

64. Lindenmair A, Hatlapatka T, Kollwig G, et al. Mesenchymal stem or stromal cells from amnion and umbilical cord tissue and their potential for clinical applications. *Cells*. 2012;1(4):1061-1088.